M2LW-23OR0402029

Light Water Reactor Sustainability Program

The Mechanism of Irradiation Assisted Stress Corrosion Cracks in Stainless Steels

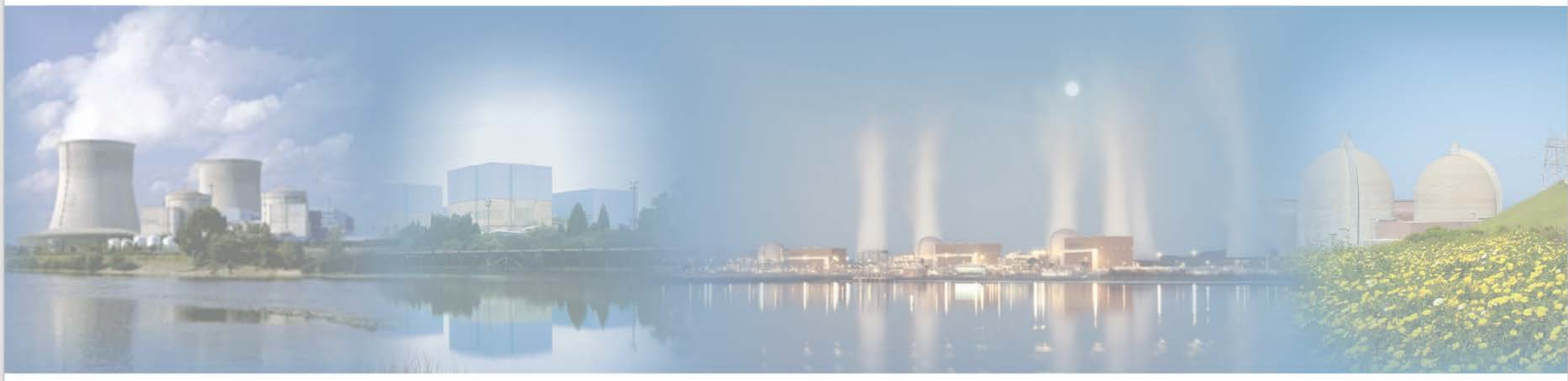

September 2023

U.S. Department of Energy

Office of Nuclear Energy

M2LW-23OR0402029

The Mechanism of Irradiation Assisted Stress Corrosion Cracks in Stainless Steels

Gary S. Was (Principal Investigator)
Abdullah Singlawi
Srinivasan Swaminathan
Kai Sun

September 2023

Prepared for the
U.S. Department of Energy
Office of Nuclear Energy

SUMMARY

The objective of this Light Water Reactor Sustainability (LWRS) project is to determine the mechanism of irradiation-assisted stress corrosion cracking (IASCC) in austenitic stainless steels in a PWR primary water environment and to propose mitigation strategies. A novel miniaturized four-point bend test was used to determine the crack initiation stress and to relate it to the microstructure features responsible for crack initiation. In this current work, we lay out the mechanism of IASCC as deduced from work in this LWRS program, complimentary programs and work done by others over the past 60 years. Despite evidence of this degradation mode that dates back to the 1960s, the mechanism by which it occurs has remained elusive. Here, using a high resolution electron backscattering technique to analyze local stress-strain states, high resolution transmission electron microscopy to identify grain boundary phases at crack tips, and decoupling the roles of stress and grain boundary oxidation, we are able to unfold the complexities of the phenomenon to reveal the mechanism by which IASCC occurs. We discuss the applicability of the findings to the IASCC of engineering alloys in the critical applications of core components in nuclear reactor cores in both current and advanced reactor concepts. As such, this report provides a mechanistic description of IASCC or why irradiation promotes intergranular stress corrosion cracking in austenitic alloys.

KEY FINDINGS

- Grain boundaries are weakened by oxidation, which can occur in the unloaded condition but is much more rapid under load.
- An amplification of the stress on the grain boundary combined with weakening of the boundary by oxidation lowers the applied stress for crack initiation to values well below the bulk yield stress of the alloy.
- While not required for crack initiation, formation of an amorphous silicon oxide phase below the initiated crack tip, promotes continued cracking down the boundary by virtue of its high solubility in high temperature water.
- Combined, these processes set up the condition for initiation of intergranular cracks at stresses well below that required to crack non-irradiated stainless steels.
- The mechanism also answers many questions regarding the conditions for IASCC.
- The mechanism also provides insight into mitigation strategies.

ACKNOWLEDGEMENT

This project was co-founded by US-DOE under the Light Water Reactor Sustainability (LWRS) program Materials Research Pathway (Contract 4000136608) and EPRI (Contract 10010367). The authors would like to thank Connor Shamberger for assistance in the Irradiated Materials Testing Laboratory at the University of Michigan. Gratitude is also extended to Dr. Maxim Gussev, Patricia Tedder, Jesse Werden and other technical support staff at Oak Ridge National Laboratory (ORNL) for assistance with specimen handling and preparation.

The Mechanism of Irradiation Assisted Stress Corrosion Cracks in Stainless Steels

1. Introduction

While having first been observed as early as 1965[1], the process by which irradiation assisted stress corrosion cracking (IASCC) occurs has remained elusive. This is due in part to the synergistic nature of its occurrence, requiring an irradiated microstructure, high temperature (280-320°C) water (corrosive), and application of stress but at levels well below the yield strength. Absent irradiation, intergranular stress corrosion cracking of austenitic stainless steels requires stresses at or above the yield strength of the alloy. Even in the sensitized condition, the stress dependence curve for IG cracking of Type 304 stainless steel is asymptotic to the at-temperature yield strength of the sensitized alloy in 288°C water containing 0.2 ppm oxygen, Figure 1.[2,3] For example, of the 93 incidents of cracking on Type 304 stainless steel recirculation and core spray lines in boiling water reactors (BWR), none were found to have occurred at stresses below the yield strength[3]. Numerous other studies have confirmed this stress dependence of cracking of austenitic stainless steels in high temperature water.[4–11]

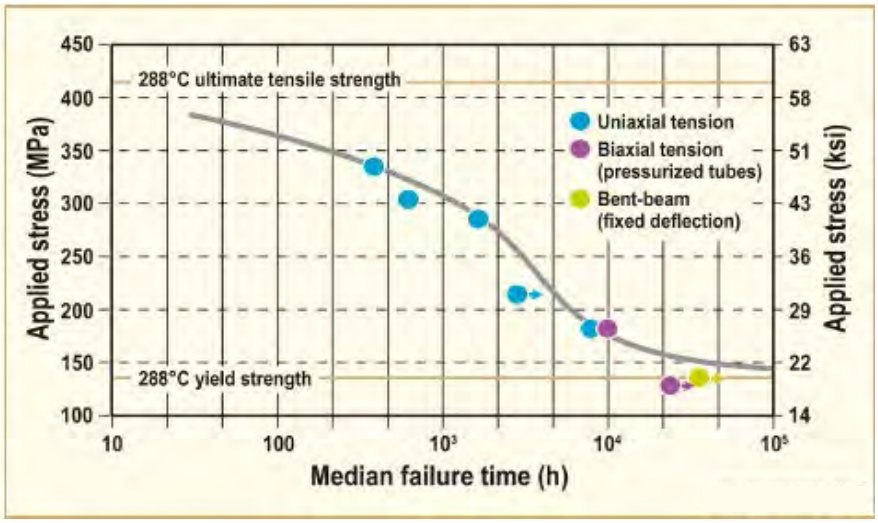

Figure 1. Stress dependence curve for IG cracking of non-irradiated sensitized type 304 stainless steel in 288°C water with 0.2 ppm oxygen.[2,3]

Absent a water environment, IG cracking of irradiated stainless steel is difficult to induce at damage levels typical of components in light water reactor cores. Straining experiments on irradiated stainless steels in inert environments at reactor core temperatures rarely produce IG cracking. Very high damage levels can induce transgranular (TG) cracking by channel fracture.[12] On rare occasion IG cracking has been reported, but only after straining into the plastic regime and the resulting %IG on the fracture surface was very low,[13–19] and the conditions that induce IG

cracking are not consistent with IASCC. Irradiation assisted stress corrosion cracking is ubiquitous in that it occurs in all LWR environments in numerous core components encompassing a wide range of austenitic stainless steels and nickel-base alloys. Failure occurs well below the at-temperature, irradiated yield strength, and the fracture surface is typically fully intergranular. Figure 2 shows the unique aspect of IASCC – that it occurs at stresses as low as 40% of the yield strength, which distinguishes it from IG cracking of non-irradiated stainless steels in high temperature water or irradiated stainless steels in high temperature inert gases.

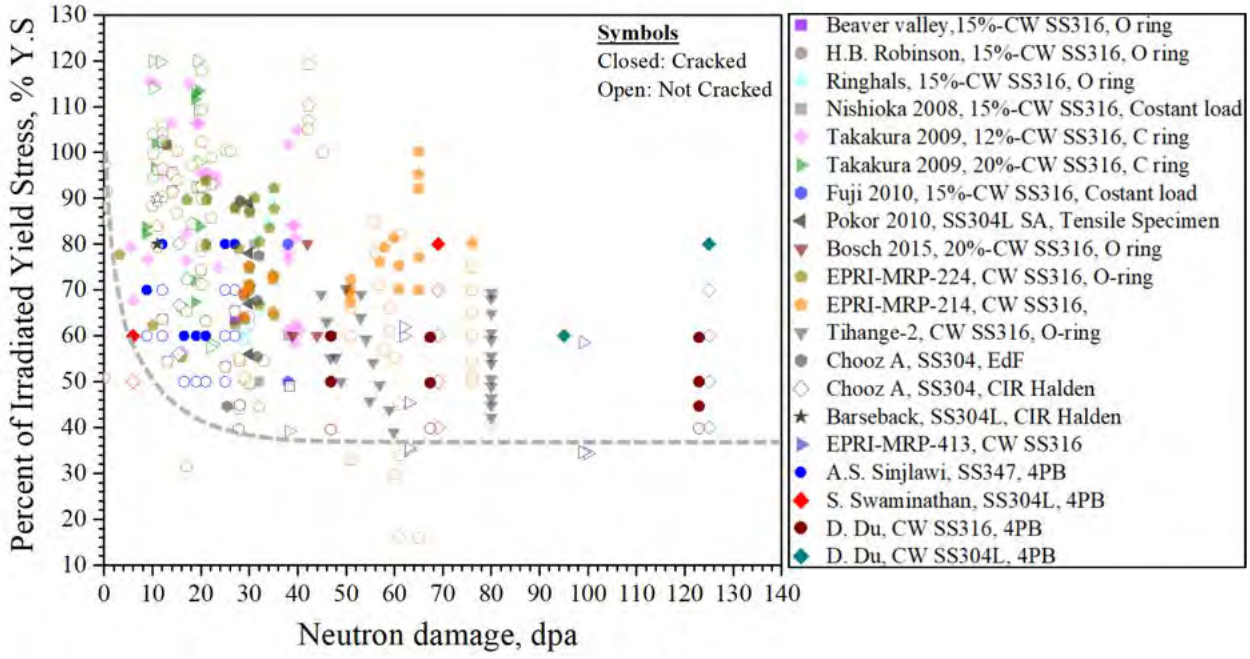

Figure 2. Plot of % of irradiated yield stress at which cracking occurs as a function of damage level for various irradiated, austenitic stainless steels strained in simulated PWR primary water.[20-25] The curve represents a bounding condition on observations of cracking.

Because IASCC is a form of intergranular stress corrosion cracking, early research focused on the phenomenon of radiation induced segregation (RIS) of major and minor/impurity elements that could degrade the strength of the grain boundary. RIS is often implicated in IASCC of stainless steels, especially in oxidizing environments, due to the wealth of data from lab and plant operational experience with sensitized components.[20–25] However, these experiments uncovered no single element that consistently correlated with increased crack initiation susceptibility[26–30] with perhaps, silicon being the one element that appeared to affect cracking. RIS-induced grain boundary chromium depletion has been suspected as a factor because of the well-known susceptibility of sensitized stainless steels. While it correlates with IG cracking, chromium depletion is inconsistent with cracking in low potential, PWR primary water. Among other features of the environment that correlate with cracking is yield strength. It is well known that yield strength is a factor in stress corrosion cracking, and in particular, in the crack growth rate of austenitic stainless steels.[20,31] Irradiation causes significant increases in the yield strength by as much as 4-5x that of the solution annealed state.[32–34] However, the physical process(es) that tie hardening to IASCC have never been identified. Yet there are three key observations that hold the answer to the IASCC mechanism. They are: 1) Grain boundaries in irradiated austenitic alloys oxidize when

exposed to high temperature water, 2) irradiated alloys deform in a completely different manner than the non-irradiated condition, and 3) silicon segregated to the grain boundary oxidizes when exposed to high temperature water. The linkage between these three factors is key to the mechanism of IASCC initiation.

2. Oxidation of grain boundaries degrades their strength

The exposure of irradiated austenitic alloys to high temperature water results in oxidation that penetrates down the grain boundary. Grain boundary oxidation is commonly observed in many nickel-base alloys in the non-irradiated state.[35–42] but rarely in the non-irradiated condition of stainless steels. Figure 3 shows examples of oxidized grain boundaries in planar and cross-section views. The grain boundary oxide formed in irradiated stainless steels in high temperature water is an iron-chromium spinel consisting of a multi-layered structure, Figure 4; iron-rich over chromium-rich over nickel-rich at the oxide-metal interface.[43–47]

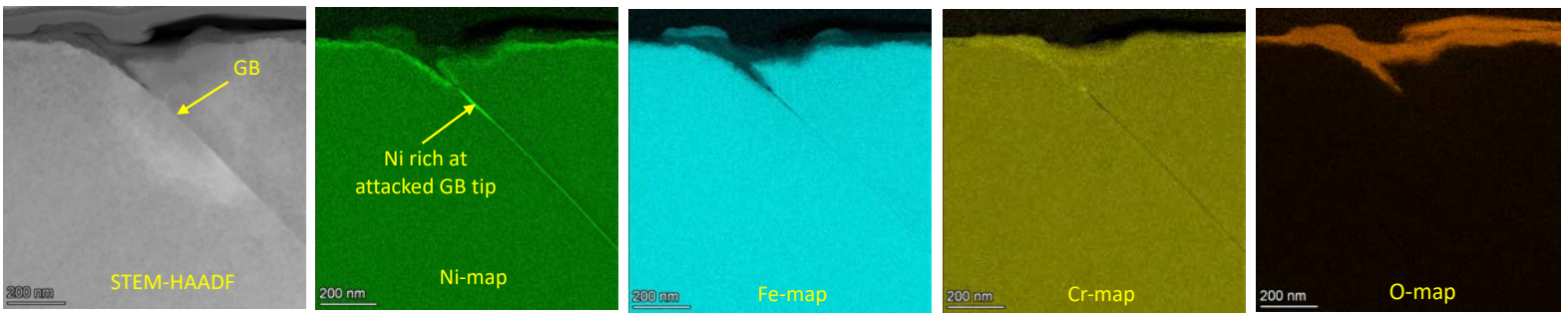

Figure 3. Examples of oxidized grain boundaries in irradiated 304L SS; a) planer view with composition profile across boundary, and b) cross sectional view with element maps.

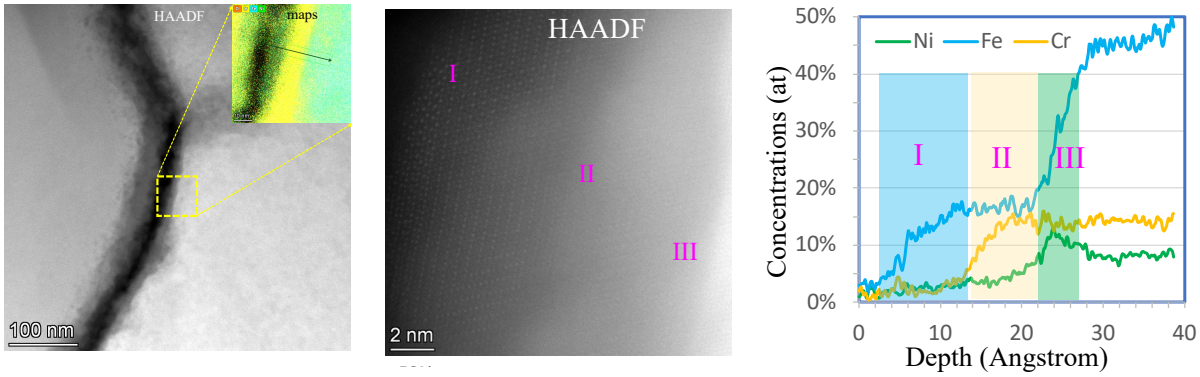

(a) (b) (c)

Figure 4. Triple layer structure of GB oxide; a) low-mag HAADF image, b) high magnification HAADF image, and c) composition profile with Fe-rich oxide over a Cr-rich oxide on a thin Ni-rich layer adjacent to the metal.

The oxide weakens the grain boundary to varying degrees depending on its structure and porosity. Measurements of the fracture strength of oxidized grain boundaries of irradiated stainless steels are difficult to make because of the need to test what is essentially the boundary of a bi-crystal. While only semi-quantitative, measurements consistently show that the stress to fracture a grain boundary progressively drops with increasing exposure to high temperature water.[48] If oxidized grain boundaries are indeed weakened and all is needed is a high enough stress to fracture, then once oxidized, they should be able to be cracked without aid of the environment. Recently, experiments that decouple stress and corrosion have shown that grain boundaries of irradiated 304 SS oxidized in water without application of stress can indeed be cracked by at stresses below yield in an inert (UHP argon) environment, Figure 5, whereas their unexposed counterparts cannot.[49] However, oxidation is greatly accelerated by stress.[49] Since irradiated stainless steels are generally not susceptible to IG cracking in inert gas below the yield stress, then the oxidized state of the grain boundary as a key factor in IASCC.

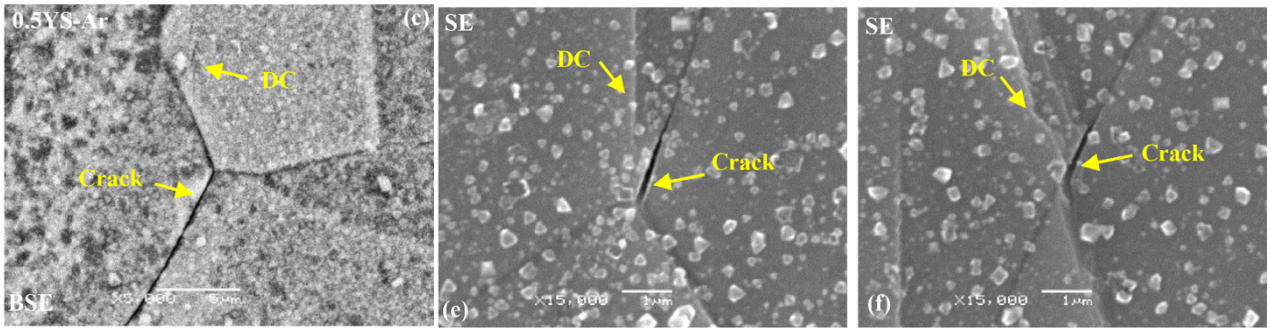

Figure 5. Cracking of previously oxidized GB of irradiated 304L after straining in ultra-high purity Ar.[49]

3. Localized deformation provides stress amplification on grain boundaries

Irradiation induced clusters are barriers to dislocation motion and result in hardening of the alloy. Once dislocations overcome the obstacles, they form channels, or stacked slip planes, through the solid, typically initiating at grain boundaries and cutting through the grain to the grain boundary, resulting in two principle options; one in which a favorable slip plane is activated in the neighboring grain, resulting in the transfer of slip to that grain (continuous dislocation channel (DC)), and one in which no such activation occurs and the channel terminates at the grain boundary (discontinuous DC). These two cases present very different strain/stress states at the dislocation channel-grain boundary (GB-DC) site. In fact, the intersection of discontinuous channels with grain boundaries has been observed to have a much higher probability of cracking than that for continuous DC-GB sites.[50] The likely cause is an increased stress at the discontinuous GB-DC site. Both computation and experiment have confirmed this result.

One of the first studies of the local stress at discontinuous DC-GB sites utilized TEM and finite element analyses of a 304L stainless steel irradiated to 0.16 dpa and strained at 290°C to initiate dislocation channels.[51] For typical values of channel aspect ratio (length/thickness), the normal stress at the grain boundary perpendicular to the loading axis is between 4 and 8 times that of the applied stress. Given that the fracture stress at high dpa is about 320 MPa.[51,52] Figure 2, the value of stress at the GB is 1.3-2.6 GPa, Figure 6a. These values agree well with large scale MD simulations that calculated the stress on the GB at a DC site is in the range 1.5 to 3.5 GPa, Figure 6b, depending on the degree of disorder of the boundary.[53,54] Experimental measurements of the local stress at DC-GB sites using high resolution electron scattering detection (HREBSD) revealed stresses between ~1 and 2 GPa in a proton irradiated Fe-13Cr-15Ni alloy deformation in high purity Ar at 288°C to produce dislocation channels. High resolution electron backscattering detection was used to measure the local strain tensor, which was then converted to a stress tensor as shown in the example in Figure 6c. In total, the local stress distributions were determined for 75 grain boundaries with discontinuous channels, Figure 6d, and 15 boundaries with continuous dislocation channels,[49] Figure 6e. Raw data is shown in blue and the fit to the Eshelby equation is shown as a solid red line.

$$\sigma = A + \frac{K}{\sqrt{r + B}}\ [GPa] \qquad (1)$$

where σ is the grain boundary normal stress, K is the stress intensity factor, r is the distance from grain boundary to the dislocation pile-up, and A and B are constants. Dashed red lines denote the upper and lower bounds of the stresses determined from HREBSD. The data confirm the MD and FE calculations of a very high local stress at discontinuous DC-GB sites. The high local stress translates into IG cracking was confirmed by subsequent slow strain rate experiments that was then conducted on the sample in 288°C. Each of the 90 grain boundaries was then inspected for cracks and the cracking probability is plotted as a function of the normal tensile stress on the grain boundary in Figure 7. Note that cracking occurs when the normal stress is above ~1.0 GPa and the probability increases monotonically with stress reaching a value of 1 at ~1.8 GPa.

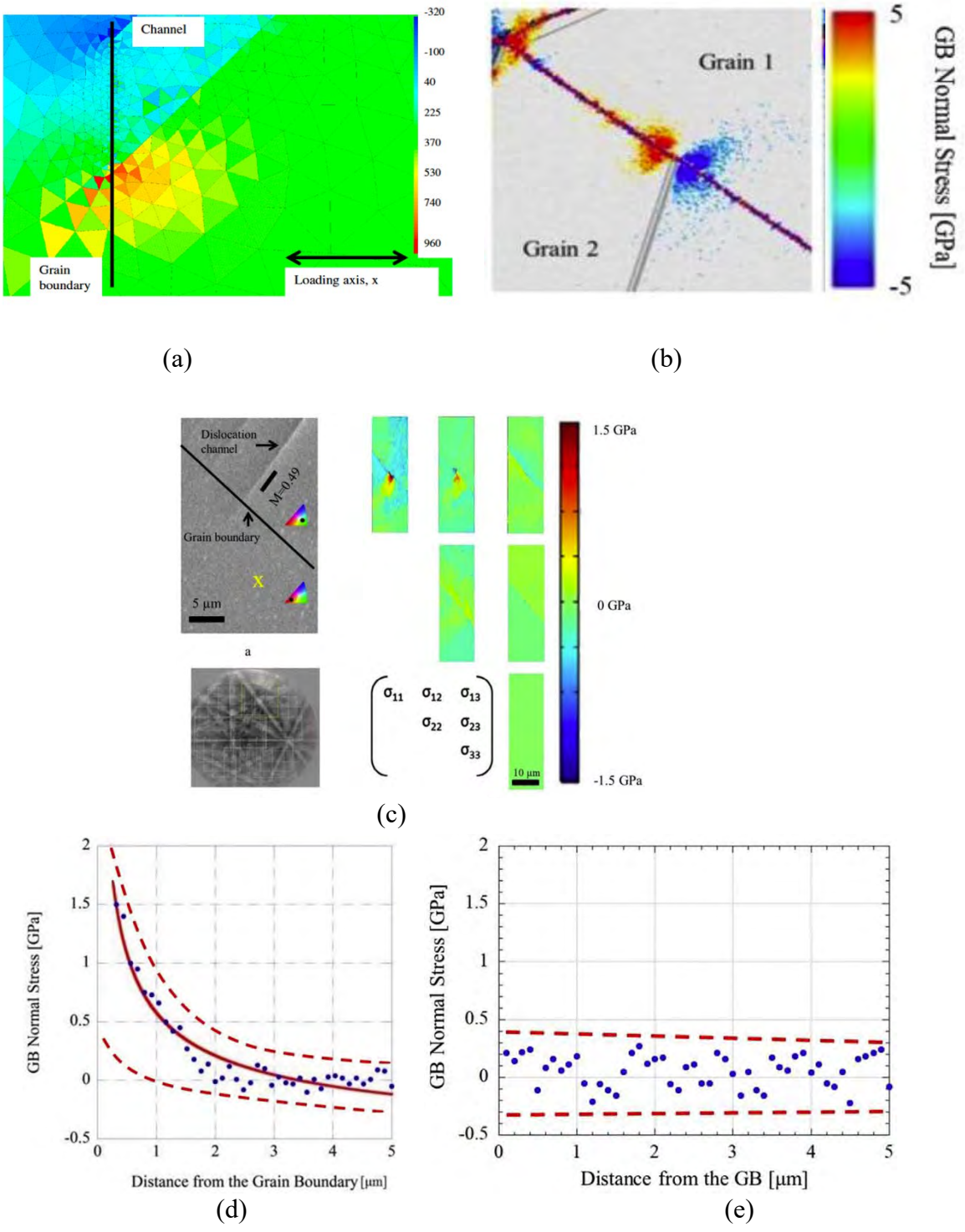

Figure 6. Computational and experimental results on local stresses at dislocation channel-grain boundary interaction sites; a) FEA model result (unit in MPa),[51] b) MD simulation,[53], c) stress tensor at DC-GB site,[54] and local stress distribution measured using HREBSD for d) discontinuous DC-GB sites,[54] and e) continuous DC-GB sites.[54] Raw data is shown in blue and the fit to the Eshelby equation is shown as a solid red line, while the dashed red lines indicate upper and lower bounds for the set of data.

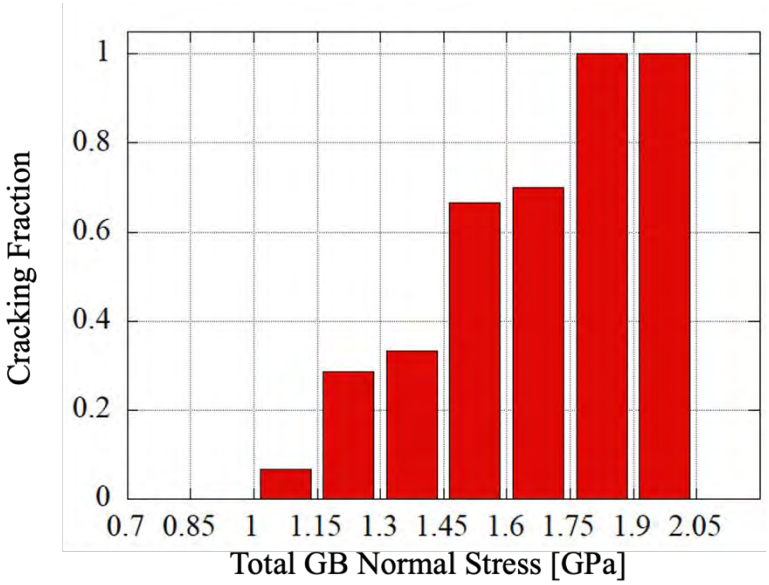

Figure 7. Probability of cracking at discontinuous DC-GB sites as a function of normal stress on the grain boundary in 304L irradiated to 5 dpa and strained in simulated BWR water.[54]

This range of values brackets the fracture stress of iron-chromium spinel measured to be 1.4-1.6 GPa by Abad et al.,[55] and 1.35 GPa determined by finite analysis of an experiment on oxidized grain boundaries in Ni-base alloy 600 by Dugdale et al.[39] Given that fracture occurs at stresses in the range 300-600 MPa,[56] well below these values for oxide fracture, there must be some additional source of stress to reach such values, and that source is the dislocation channels that terminate at the grain boundary. Figure 8 shows several cracks along grain boundaries in irradiated alloys 347 (a, b, c), 316 (d) and 304 (e) strained incrementally in simulated PWR primary water containing 1000 ppm B as H_3BO_3, 2 ppm Li as LiOH and 3 ppm H at 320°C. Note the tortuous fracture path through the oxide, as opposed to the oxide-metal interface. While grain boundaries can oxidize without the aid of stress, the application of stress greatly increases the extent of grain boundary oxidation as shown by the graph in Figure 9 for 304L stainless steel. The strength degradation of the grain boundary due to oxidation combined with enhancement of the local stress at DC-GB sites provides the condition for initiation of intergranular cracks.

4. Silicon contributes to crack extension down the grain boundaries

Yet there is an additional factor in the mechanism of IASCC that can enhance the cracking susceptibility of some irradiated stainless steels. As noted earlier, significant data exists to indicate that silicon may play a role in IASCC. Constant extension rate tests were conducted on a high purity heat of Fe-18Cr-12N-1Mn-0.02C and one with the same composition and 1.05 wt% Si following irradiation with 3.2 MeV protons to 5.5 dpa at 360°C.[27] Samples were pulled at a strain rate of 3.5×10^{-7} s^{-1} in both simulated BWR water at 288°C and PWR primary water at 320°C. In BWR water, the Si-containing sample had almost double the %IG on the fracture surface, and 4 times the number of cracks on the gage section over the high purity sample. In PWR PW, the Si-containing sample had 54 IG cracks vs. none on the high purity sample, Figure 10. A series of

heats of stainless steels and nickel-base alloys with varying Si content were strained in simulated PWR primary water and revealed that in a 15Cr-50Ni-xSi alloy, the %IG on the fracture surface increased dramatically at a Si concentration of about 1 wt%, Figure 11a.[57,58] Silicon had the same effect in crack growth tests on 304L SS containing various levels of Si conducted in high temperature water. At low potential, an increase in Si from 2% to 6% resulted in an increase in crack growth rate by more than a factor of 10 in one study, Figure 11b.[59] In another study, CGR tests of a Fe-28Ni-12Cr-xSi alloy found that an increase in Si from 0 to 2.5 wt% resulted in an increase in the CGR by a factor of 22, Figure 11c.[60]

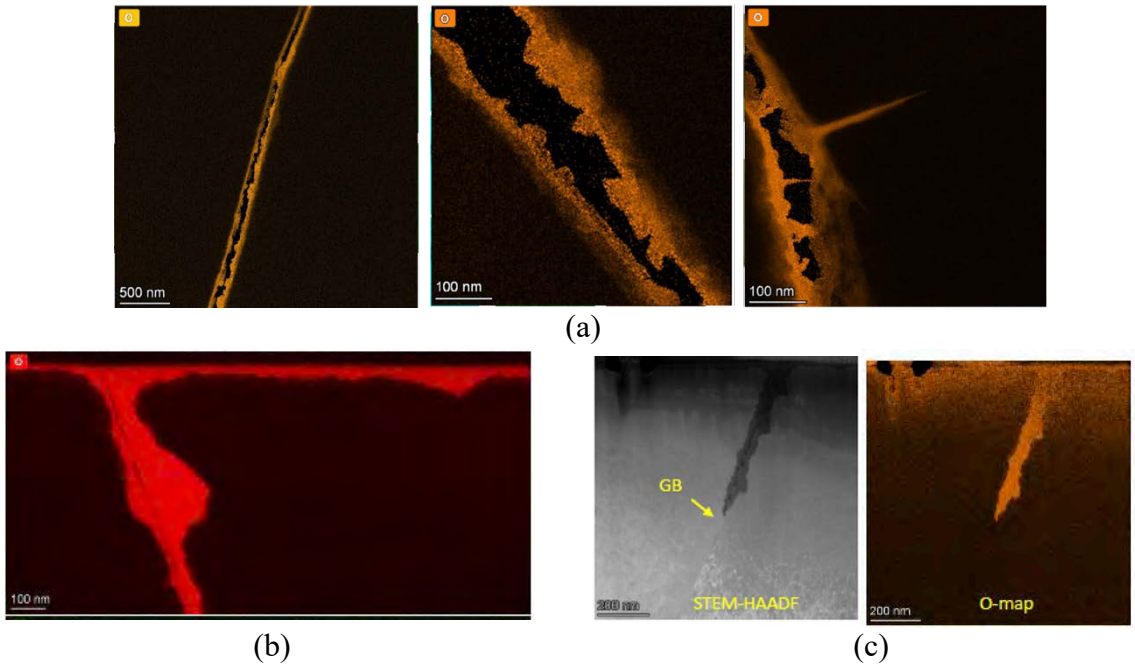

Figure 8. Fractured grain boundaries in a) irradiated 347 SS, b) irradiated CW316L SS and c) irradiated 304L SS, all strained,[49] in simulated PWR primary water at 320°C.

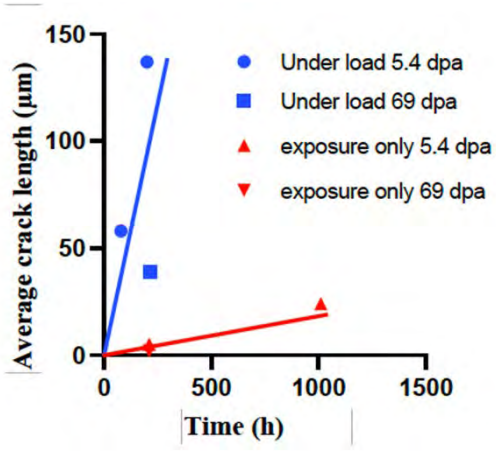

Figure 9. The effect of stress on the depth of the grain boundary oxide[58] for the cases of straining in 320°C water (●■), and exposing in 320°C water and subsequently straining in 320°C argon (▲▼).

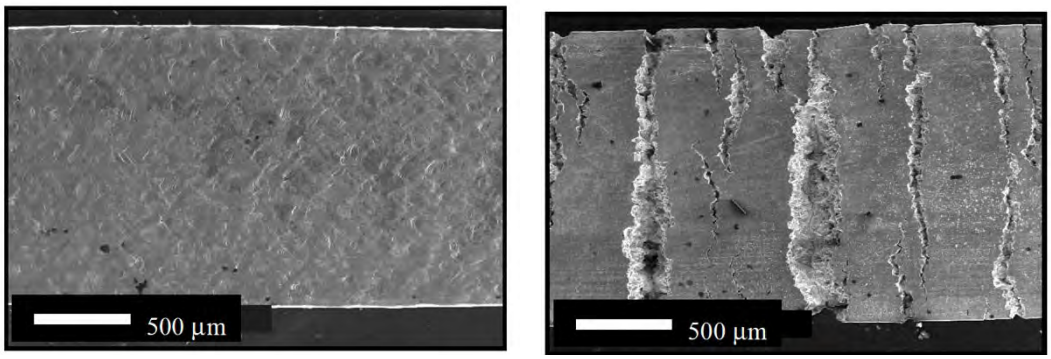

(a) (b)

Figure 10. IG cracking in model alloys; a) Fe-18Cr-12Ni-1Mn, and b) Fe-18Cr-12Ni-1Mn-1Si irradiated to 5 dpa and strained to failure in 288°C simulated BWR normal water chemistry.[27]

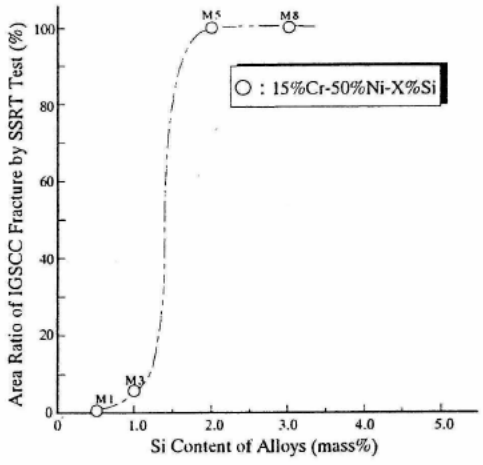

(a)

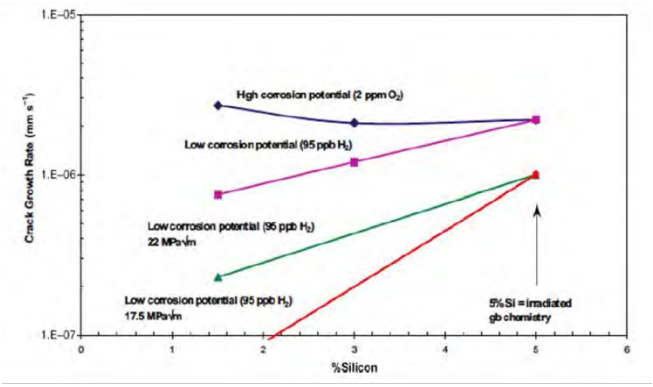

(b)

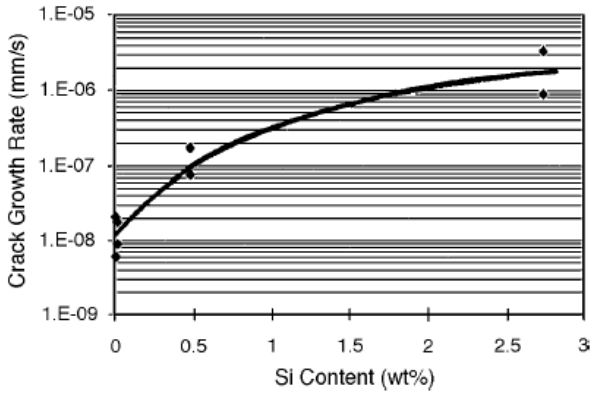

(c)

Figure 11. Effect of Si: a) %IG fracture in SSRT tests on 15Cr-50Ni-XSi in simulated PWR primary water,[58] *b) crack growth rate tests on 304L SS in 288°C pure water,*[59] *and c) crack growth rate tests on Fe-28Ni-12Cr-xSi in 325°C PWR primary water.*[60]

But the mechanism by which Si affects IASCC has not been explained to date. High resolution TEM analysis of crack tips in high Si, Type 347 SS strained in PW primary water provides insight into the process. Figure 12 shows a high resolution image of the crack tip of a 347 sample. The tip is approximately 50 nm below the surface. Note the lattice planes on each side of the tip. Below the crack tip is an oxidized region approximately 2-3 nm wide and extending ~50 nm down the grain boundary. Penders et al.,[61,62] also observed an oxidized region beyond the crack tip in fractured O-ring samples of CW 316L SS. Here we have identified the oxide as an amorphous silicon oxide, a-SiO_x. The EDS maps of Ni, Si and O show that beyond the depth of penetration of oxygen (line 3), the boundary is enriched in both Ni and Si due to radiation induced segregation. Above the tip (line 0), Ni is enriched at the oxide-matrix interface and Si is absent. The amorphous SiO_x region lies between lines 1 and 2, as evidenced by the very strong Si and O signals and the partitioning of Ni to the oxide-metal interface. As amorphous silica is soluble in high temperature water,[63,64] its dissolution provides a pathway for the crack to propagate down the boundary. While not required for IASCC, silicon enrichment at the grain boundary augments the susceptibility of the alloy to IASCC initiation and perhaps, propagation. By comparison, the 304L sample with low Si content is also susceptible to IASCC but no such phase was formed at the grain boundary. Thus, silicon enhances the susceptibility to IASCC but is not necessary for it to occur.

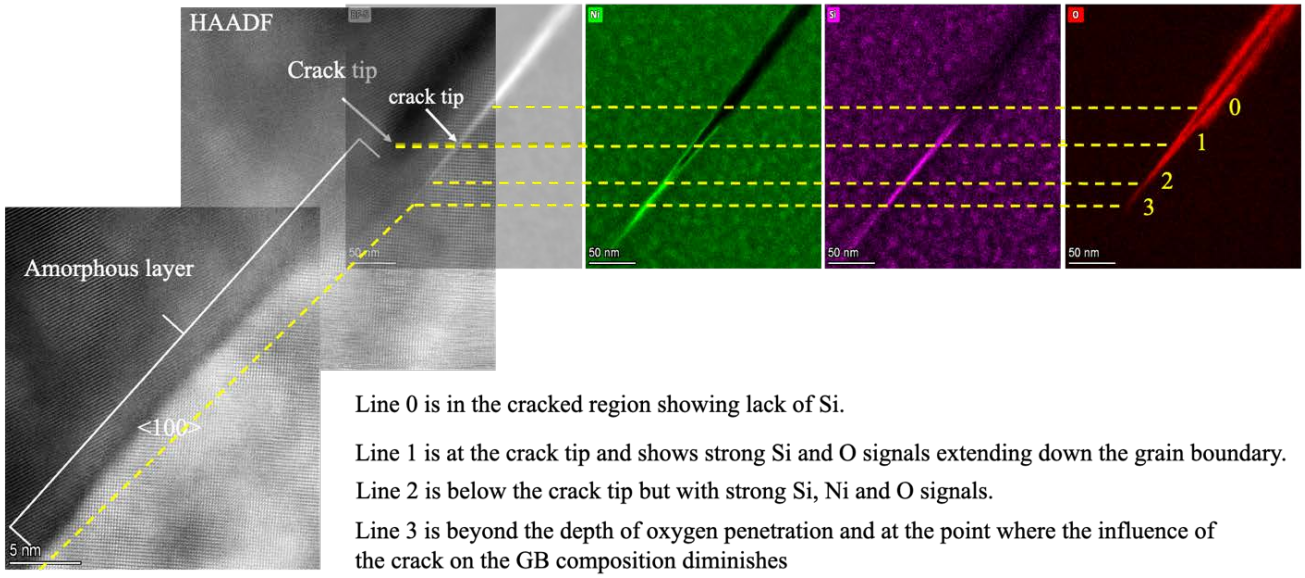

Figure 12. High resolution transmission electron microscopy image and accompanying composition maps of a crack tip in 347 SS irradiated to 26.4 dpa and strained to 60% of the irradiated yield stress in KOH at 320°C showing amorphous silicon oxide (a-SiO_x) extending over 50 nm beyond the crack tip and down the grain boundary.

5. Outstanding questions on IASCC

With an understanding of how IASCC occurs, a number of questions regarding IASCC observations made over decades can be addressed, such as: *Why an irradiated alloy is so susceptible to IASCC? How can cracking occur below the yield point? Why does cracking correlate with yield strength? Why does cracking susceptibility increase with dpa but only up to a point? How can IASCC occur in a constant load test? What about cold worked condition in which DCs don't readily form? Why don't all boundaries crack?*

What makes the irradiated condition so susceptible to IASCC is the mode of deformation that results in dislocation channels that create a high local stress on an oxidized grain boundary. Cracking can occur well below the yield point because plasticity can occur very locally in the form of dislocation channels. At low stresses, the density of channels is very low, but there are enough to create stress points at oxidized boundaries to induce formation of a crack. IASCC correlates with yield strength because yield strength increases with damage level, increasing the degree of deformation localization channels. However, once the irradiation microstructure saturates, so does the yield strength and therefore, the localization of deformation. In a rising load test such as the CERT or SSRT, channel formation increases with stress producing increasing numbers of discontinuous DC-GB sites for crack nucleation. In a constant load test, the load doesn't change, but the state of the grain boundaries changes due to oxidation, which degrades GB strength and increases the susceptibility to IG crack initiation. Cold worked stainless steels also fail by IASCC, but dislocation channels are not often observed. Rather, the deformation bands formed during cold working likely serve in much the same role as DCs. The intersection of these deformation bands with grain boundaries have been found to be sites of increased oxidation and crack initiation[38,49,61,62,65] and potentially increased stress,[66] Figure 13.

The big question is the following: Why don't all boundaries crack? Since cracking relies on a critical stress at a susceptible (oxidized) grain boundary, a number of conditions must be fulfilled. First, a channel must be formed. That channel must terminate at a grain boundary rather than transmit slip to the neighboring grain. The boundary must be oriented so as to maximize the local stress at the DC intersection site. The boundary must be oxidized, and importantly, the channel must intersect an oxidized grain boundary near the surface to initiate an IG crack. Thus, the number of conditions that must be fulfilled means that IASCC is a rather rare occurrence such that only a small fraction of grain boundaries will fail for any given set of environmental conditions. It is not surprising that because of the interplay of so many factors, probabilistic approaches are often employed to explain IASCC.[67] While there will always be exceptions, the mechanism described here provides both a qualitative and quantitative description of the processes that govern IASCC in irradiated stainless steels. With this deeper understanding of the IASCC process, mitigation measures and physically-based predictive models can now be developed to both control IASCC and to avoid its occurrence.

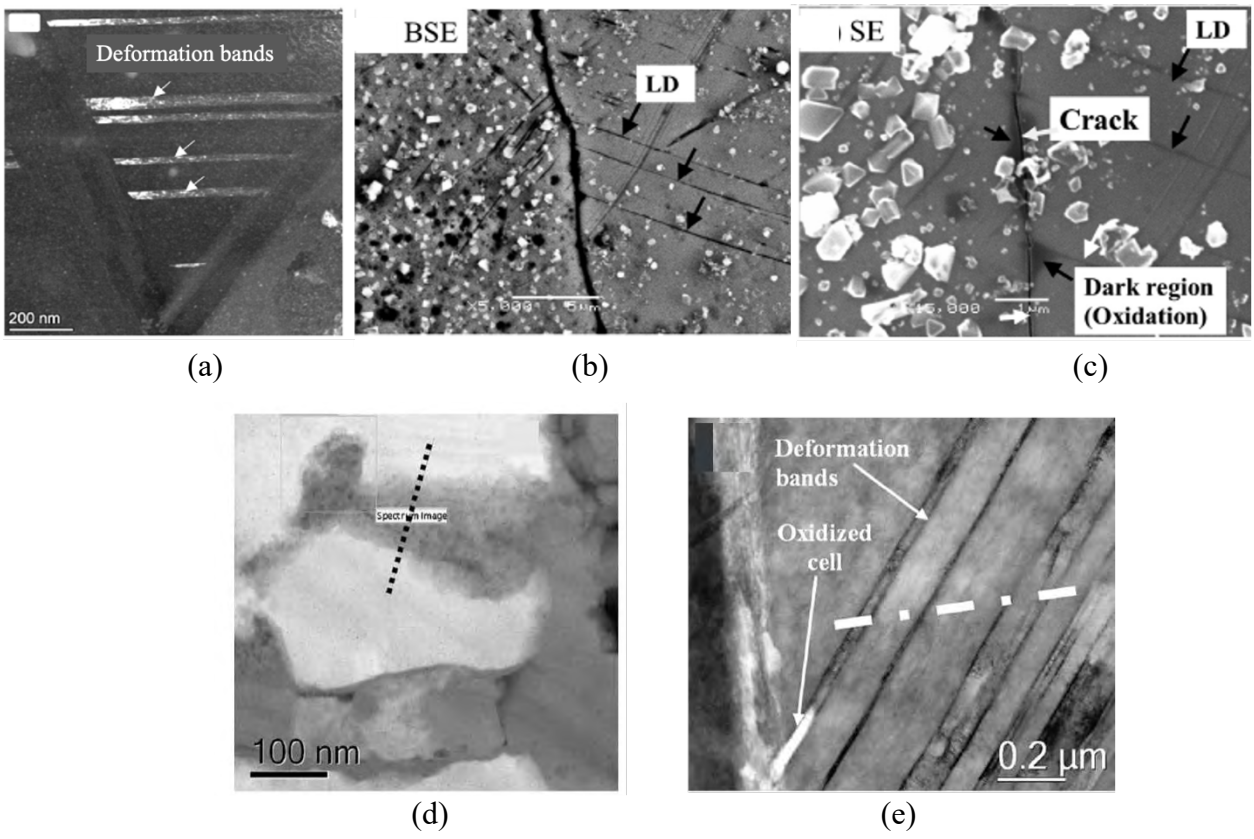

Figure 13. Localized deformation (LD) bands in CW 316SS irradiated to 125 dpa at 320°C and strained to 0.6σ_y in simulated PWR primary water (a-c), and in CW 304SS[47] (d,e).

6. Summary

The key processes that drive IASCC in irradiated stainless steels, depicted in Figure 14, interact in the following way: Grain boundaries oxidize with the oxides forming spinel structures down the boundary for hundreds of nm to several micrometers, Figure 14a. Tensile stress enhances the rate of grain boundary oxidation, thus weakening the boundary as the fracture strength of the boundary drops to the ~1 GPa regime and potentially lower, depending on the porosity of the oxide Figure 14b. Application of stress induces plasticity on a very localized scale at applied stresses well below the general irradiated, at-temperature yield strength of the alloy. The localized deformation in the form of dislocation channels spreads across the grain and either transfers strain to the neighboring grain, or terminates at the grain boundary. In the latter case, the local stress at the DC-GB site can increase to the ~1GPa level and higher, sufficient to nucleate a crack in the near surface region of an oxidized (weakened) grain boundary, Figure 14c. The oxide fractures, allowing for oxidation of the boundary beneath the crack tip to induce propagation of the crack. In cases where Si is enriched at the grain boundary by radiation induced segregation, the silicon oxidizes to form an amorphous silica layer at the boundary several nm wide and hundreds of nm below the crack tip. By virtue of its solubility in high temperature water, a-silica dissolves, aiding the extension at the crack tip and providing for oxidation of Si further down the boundary, Figure 14d.

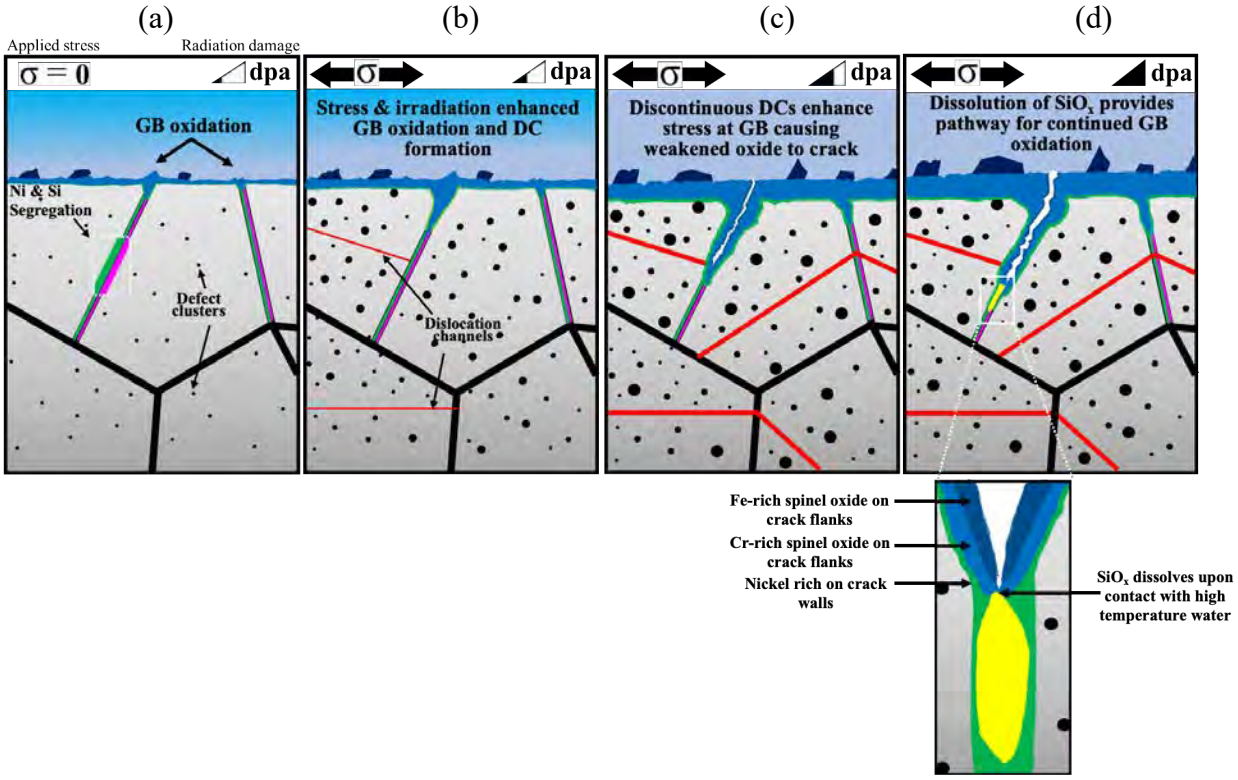

Figure 14. Schematic of the processes driving IASCC: a) irradiation-induced defect cluster formation, segregation of minor and major alloying elements to grain boundaries, and grain boundary oxidation at low damage level, b) application of stress combined with increased irradiation damage enhances grain boundary oxidation and induces formation of dislocation channels, c) dislocation channels impinging on GBs near the surface cause fracture of the weak oxidized grain boundaries, and d) exposure of Si-enriched GBs to water oxidizes the Si to amorphous SiO_x that dissolves, providing a pathway for continued oxidation of the boundary, setting up the conditions for crack growth.

7. References

1. Duncan, R. N. *et al.* Stainless-Steel-Clad Fuel Rod Failures. *Nuclear Applications* **1**, 413–418 (1965).
2. Ford, F. P. , G. B. M. . H. R. M. Corrosion in Boiling Water Reactors. in *ASM Handbook Corrosion* vol. 1c3 344–345 (ASM, 2006).
3. Gordon, B. M. *Corrosion and Corrosion Control in BWRs, General Electric Resport NEDO-24819A Class 1*. (1984).
4. Chang., L., Burke, M. G. & Scenini, F. Stress corrosion crack initiation in machined type 316L austenitic stainless steel in simulated pressurized water reactor primary water . *Corros Sci* **138**, 54–65 (2018).
5. Scenini, F. , *et al.* Oxidation and SCC Initiation Studies of Type 304L SS in PWR Primary Water. in *Proc. 18th Int'l Conf. Environmental Degradation of Materials in Nuclear Power Systems – Water Reactors* 793–810 (2019).
6. Lozano-Perez, S., Dohr, J., Meisnar, M. & Kruska, K. SCC in PWRs: Learning from a Bottom-Up Approach. *Metallurgical and Materials Transactions E* **1**, 194–210 (2014).
7. Liu, X. *et al.* Toward the multiscale nature of stress corrosion cracking. *Nuclear Engineering and Technology* vol. 50 1–17 Preprint at https://doi.org/10.1016/j.net.2017.10.014 (2018).
8. Karlsen, W., Diego, G. & Devrient, B. Localized deformation as a key precursor to initiation of intergranular stress corrosion cracking of austenitic stainless steels employed in nuclear power plants. *Journal of Nuclear Materials* **406**, 138–151 (2010).
9. Andresen, P. L. Stress corrosion cracking of current structural materials in commercial nuclear power plants. *Corrosion* **69**, 1024–1038 (2012).
10. Zhong, X., Bali, S. C. & Shoji, T. Accelerated test for evaluation of intergranular stress corrosion cracking initiation characteristics of non-sensitized 316 austenitic stainless steel in simulated pressure water reactor environment . *Corr. Sci.* **115**, 106–117 (2017).
11. Zhong, X., Bali, S. C. & Shoji, T. Effects of dissolved hydrogen and surface condition on the intergranular stress corrosion cracking initiation and short crack growth behavior of non-sensitized 316 stainless steel in simulated PWR primary water. *Corr. Sci.* **118**, 143–157 (2017).
12. Bloom, E. E. *Radiation Damage in Metals*. (American Society for Metals, 1976).
13. Manahan, M. P., Kohli, R., Santucci, J. & Sipush, P. *A PHENOMENOLOGICAL INVESTIGATION OF IN-REACTOR CRACKING OF TYPE 304 STAINLESS STEEL CONTROL ROD CLADDING*. *Nuclear Engineering and Design* vol. 113 (1989).
14. Onchi, T. *et al.* Fractographic and microstructural characterization of irradiated 304 stainless steel intergranularly fractured in inert gas. *Journal of Nuclear Materials* **320**, 194–208 (2003).
15. Furutani, G., Nakajima, N., Konishi, T. & Kodama, M. *Stress corrosion cracking on irradiated 316 stainless steel*. www.elsevier.nl/locate/jnucmat.
16. Matsuoka, T. *et al.* Intergranular cracking in cladding tube of PWR RCCA Rodlets. *JSME Int'l J.* **38**, 515–523 (1995).
17. Fukuya, K. *et al.* Fracture behavior of austenitic stainless steels irradiated in PWR. *Journal of Nuclear Materials* **378**, 211–219 (2008).

18. Fukuya, K., Nakano, M., Fujii, K. & Torimaru, T. IASCC susceptibility and slow tensile properties of highly-irradiated 316 stainless steels. *J. Nucl. Sci. Technol.* **41**, 673–681 (2004).
19. Morisawa, J. *et al. Hydrogen analysis and slow strain rate test in Ar gas for irradiated austenitic stainless steel*. www.elsevier.nl/locate/jnucmat.
20. Bruemmer, S. M. *et al.* Radiation-induced material changes and susceptibility to intergranular failure of light-water-reactor core internals. *Journal of Nuclear Materials* **274**, (1999).
21. Scott, P. M. A review of irradiation assisted stress corrosion cracking. *J. Nucl. Mater.* **211**, 101–122 (1994).
22. Brown, K. S. & Gordon, G. M. Effects of BWR Coolant Chemistry on the Propensity for IGSCC Initiation and Growth in Creviced Reactor Internals Components. in *Proc. 3rd Environmental Degradation of Materials in Nuclear Power Systems—Water Reactors* 243–248 (The American Institute of Mining, Metallurgical, and Petroleum Engineers , 1988).
23. Horn, R. M., Gordon, G. M., Ford, F. P. & Cowan, R. L. *Experience and assessment of stress corrosion cracking in L-grade stainless steel BWR internals*. *Nuclear Engineering and Design* vol. 174 (1997).
24. Nelson, J. L. & Andresen, P. L. Review of Current Research and Understanding of Irradiation-Assisted Stress Corrosion Cracking. in *Proc. 5th Int. Symp. on Environmental Degradation of Materials in Nuclear Power Systems—Water Reactors* (eds. Cubicciotti, D., Simonen, E. P. & Gold, R.) 10–26 (American Nuclear Society, Inc., 1992).
25. Was, G. S. *et al.* Microchemistry and microstructure of proton-irradiated austenitic alloys: toward an understanding of irradiation effects in LWR core components. *Journal of Nuclear Materials* **270**, (1999).
26. Simonen, E. P., Jones, R. H. & Bruemmer, S. M. *Radiation effects on grain boundary chemistry relevant to stress corrosion cracking of stainless steels*. *Journdl of Nuclear Matermls* (1992).
27. Busby, J. T., Was, G. S. & Kenik, E. A. Isolating the effect of radiation-induced segregation in irradiation-assisted stress corrosion cracking of austenitic stainless steels. *Journal of Nuclear Materials* **302**, (2002).
28. Chung, H. M. *et al. Irradiation-assisted stress corrosion cracking of austenitic stainless steels: recent progress and new approaches*. *Journal of Nuclear Materials* vol. 239 (1996).
29. Miwa, Y. *et al. Effect of minor elements on irradiation assisted stress corrosion cracking of model austenitic stainless steels*. *Journal of Nuclear Materials* (1996).
30. Nakano, J., Miwa, Y., Kohya, T. & Tsukada, T. Effects of silicon, carbon and molybdenum additions on IASCC of neutron irradiated austenitic stainless steels. in *Journal of Nuclear Materials* vols 329–333 643–647 (2004).
31. Speidel, M. O. & Magdowski, R. Stress corrosion cracking of stabilized austenitic stainless steels in various types of nuclear power plants. in *Proc. 9th International Symposium on Environmental Degradation of Materials in Nuclear Power Systems – Water Reactors* (eds. Ford, F. P., Bruemmer, S. M. & Was, G. S.) 325–329 (Metallurgical Society of the American Institute of Mining, Metallurgical, and Petroleum Engineers , 1999).

32. Singh, B. N., Foreman, A. J. E. & Trinkaus, H. *Radiation hardening revisited: role of intracascade clustering*. *Journal of Nuclear Materials* vol. 249 (1997).
33. Bruemmer, S. M., Cole, J. I., Brimhall, J. L., Carter, R. D. & Was, G. S. Radiation hardening effects on localized deformation and stress corrosion cracking of stainless steels. in (1993).
34. Lucas, G. E. *The evolution of mechanical property change in irradiated austenitic stainless steels*. *Journal of Nuclear Materials* vol. 206 (1993).
35. Fujii, K., Miura, T., Nishioka, H. & Fukuya, K. Degradation of grain boundary strength by oxidation in alloy 600. in *15th International Conference on Environmental Degradation* (eds. Busby, J., Ilevbare, G. & Andresen, P.) 1447–1458 (The Minerals, Metals & Materials Society, 2011).
36. Persaud, S. Y., Korinek, A., Huang, J., Botton, G. A. & Newman, R. C. Internal oxidation of Alloy 600 exposed to hydrogenated steam and the beneficial effects of thermal treatment. *Corros Sci* **86**, 108–122 (2014).
37. Persuad, S. Y., Ramamurthy, S. & Newman, R. C. Internal oxidation of alloy 690 in hydrogenated steam. *Corr. Sci.* **90**, 606–613 (2015).
38. Lozano-Perez, S. *et al.* Multi-scale characterization of stress corrosion cracking of cold-worked stainless steels and the influence of Cr content. *Acta Mater* **57**, 5361–5381 (2009).
39. Dugdale, H., Armstrong, D. E. J., Tarleton, E., Roberts, S. G. & Lozano-Perez, S. How oxidized grain boundaries fail. *Acta Mater* **61**, 4707–4713 (2013).
40. Bertali, G., Scenini, F. & Burke, M. G. The effect of residual stress on the Preferential Intergranular Oxidation of Alloy 600. *Corros Sci* **111**, 494–507 (2016).
41. Volpe, L., Burke, M. G. & Scenini, F. Understanding the role of Diffusion Induced Grain Boundary Migration on the preferential intergranular oxidation behaviour of Alloy 600 via advanced microstructural characterization. *Acta Mater* **175**, 238–249 (2019).
42. Vo, H. T. *et al.* Development of microscale bicrystal tensile testing for strength measurement of oxidized grain boundaries of alloy 600 exposed to PWR environments. *Materials Science and Engineering: A* **815**, 141197 (2021).
43. Terachi, T., Yamada, T., Arioka, K. & Lozano-Perez, S. *Role of Corrosion in LPSCC of Fe-and Ni-Based Alloys*.
44. Fukumura, T., Fukuya, K., Fujii, K., Miura, T. & Kitsunai, Y. Grain boundary oxidation of neutron irradiated stainless steels in simulated PWR water. in *Minerals, Metals and Materials Series* vol. Part F11 937–947 (Springer International Publishing, 2018).
45. Heuser, B. J., Li, Z., Bai. X-M., Zhong, W. & Sutton, B. J. Irradiation-assisted cracking of SA508-304L weldments with 308L groove filler and 309L butter in hot water immersion constant rate extension tests. *J. Nucl. Mater.* **581**, 54472 (2023).
46. Matthews, R. P., Knusten, R. D., Westraadt, J. E. & Couvant, T. Intergranular oxidation of 316L stainless steel in the PWR primary water environment. *Corros Sci* **125**, 175–183 (2017).
47. Lozano-Perez, S., Kruska, K., Iyengar, I., Terachi, T. & Yamada, T. The role of cold work and applied stress on surface oxidation of 304 stainless steel. *Corros Sci* **56**, 78–85 (2012).
48. Miura, T., Fujii, K. & Fukuya, K. Characterization of fracture behavior of oxidized grain boundary in neutron-irradiated stainless steel. *INSS Journal* **25**, 102–109 (2018).
49. Swaminathan, S., Sun, K. & Was, G. S. Decoupling the roles of grain boundary oxidation and stress in IASCC of neutron-irradiated 304L stainless steel. *Journal of Nuclear Materials* **585**, 154604 (2023).

50. McMurtrey, M. D., Was, G. S., Patrick, L. & Farkas, D. Relationship between localized strain and irradiation assisted stress corrosion cracking in an austenitic alloy. *Materials Science and Engineering: A* **528**, 3730–3740 (2011).
51. Sauzay, M., Bavard, K. & Karlsen, W. TEM observations and finite element modelling of channel deformation in pre-irradiated austenitic stainless steels – Interactions with free surfaces and grain boundaries. *Journal of Nuclear Materials* **406**, 152–165 (2010).
52. Bosch, R. W., Vankeerberghen, M., Gérard, R. & Somville, F. Crack initiation testing of thimble tube material under PWR conditions to determine a stress threshold for IASCC. *Journal of Nuclear Materials* **461**, 112–121 (2015).
53. Kuhr, B., Farkas, D., Robertson, I. M., Johnson, D. & Was, G. Stress Localization Resulting from Grain Boundary Dislocation Interactions in Relaxed and Defective Grain Boundaries. *Metallurgical and Materials Transactions A* **51**, 667–683 (2020).
54. Johnson, D. C., Kuhr, B., Farkas, D. & Was, G. S. Quantitative linkage between the stress at dislocation channel – Grain boundary interaction sites and irradiation assisted stress corrosion crack initiation. *Acta Mater* **170**, 166–175 (2019).
55. Abad, M. D. *et al.* Evaluation of the Mechanical Properties of Naturally Grown Multilayered Oxides Formed on HCM12A Using Small Scale Mechanical Testing. *Oxidation of Metals* **84**, 211–231 (2015).
56. Fyfitch, S., Davidsaver, S. & Amberge, K. Irradiation-Assisted Stress Corrosion Cracking Initiation Screening Criteria for Stainless Steels in PWR Systems. in *Proceedings of the 18th International Conference on Environmental Degradation of Materials in Nuclear Power Systems – Water Reactors* (ed. Jackson, J. H.) 995–1004 (2018). doi:10.1007/978-3-319-68454-3_72.
57. Fujimoto, K., Yonezawa, T., Iwamura, T., Ajiki, K. & Urata, S. Simulation of radiation induced segregation and PWSCC susceptibility for austenitic stainless steels. *Corrosion Engineering* **49**, 701–720 (2000).
58. Yonezawa, T. *et al.* Investigation of irradiation-induced intergranular stress corrosion cracking susceptibility of austenitic stainless steels for PWR by simulated radiation-induced segregation materials. *Corrosion Engineering* **49**, 655–667 (2000).
59. Andresen, P. L. & Morra, M. M. *EFFECTS OF SI ON SCC OF IRRADIATED AND UNIRRADIATED STAINLESS STEELS AND NICKEL ALLOYS.*
60. Li, G. F., Kaneshima, Y. & Shoji, T. Effects of Impurities on Environmentally Assisted Crack Growth of Solution-Annealed Austenitic Steels in Primary Water at 325°C. *CORROSION* **56**, 460–469 (2000).
61. Penders, A. G. *et al.* Microstructural investigation of IASCC crack tips extracted from thimble tube O-ring specimens. *Journal of Nuclear Materials* **565**, 153727 (2022).
62. Penders, A. G. *et al.* Characterization of IASCC crack tips extracted from neutron-irradiated flux thimble tube specimens in view of a probabilistic fracture model. *Journal of Nuclear Materials* **571**, 154015 (2022).
63. Fournier, R. O. & Rowe, J. J. The solubility of amorphous silica in water at high temperatures and high pressures. *American Mineralogist* **62**, 1052–1056 (1977).
64. Fournier, R. O. & Marshall, W. L. Calculation of amorphous silica solubilities at 25” to 300°C and apparent cation hydration numbers in aqueous salt solutions using the concept of effective density of water*. *Geochim Cosmochim Acta* **47**, 587–596 (1983).

65. Cissé, S., Laffont, L., Lafont, M. C., Tanguy, B. & Andrieu, E. Influence of localized plasticity on oxidation behaviour of austenitic stainless steels under primary water reactor. *Journal of Nuclear Materials* **433**, 319–328 (2013).
66. Du, D., Sun, K. & Was, G. S. IASCC of neutron irradiated 316 stainless steel to 125 dpa. *Mater Charact* **173**, (2021).
67. Konstantinović, M. J. Internal oxidation and probabilistic fracture model of irradiation assisted stress corrosion cracking in stainless steels. *Journal of Nuclear Materials* **495**, 220–224 (2017).